0022-3565/10/3323-785–794$20.00
THE JOURNAL OF PHARMACOLOGY AND EXPERIMENTAL THERAPEUTICS
JPET 332:785–794, 2010
Copyright © 2010 by The American Society for Pharmacology and Experimental Therapeutics
Vol. 332, No. 3
153049/3559439
Printed in U.S.A.

The Journal of PHARMACOLOGY And Experimental Therapeutics

3-(2,4-Dichlorophenyl)-4-(1-methyl-1*H*-indol-3-yl)-1*H*-pyrrole-2,5-dione (SB216763), a Glycogen Synthase Kinase-3 Inhibitor, Displays Therapeutic Properties in a Mouse Model of Pulmonary Inflammation and Fibrosis

Carmela Gurrieri, Francesco Piazza, Marianna Gnoato, Barbara Montini, Lucia Biasutto, Cristina Gattazzo, Enrico Brunetta, Anna Cabrelle, Francesco Cinetto, Raffaele Niero, Monica Facco, Spiridione Garbisa, Fiorella Calabrese, Gianpietro Semenzato, and Carlo Agostini

Department of Clinical and Experimental Medicine, Clinical Immunology and Hematology Branches, and Venetian Institute of Molecular Medicine, Centro di Eccellenza per la Ricerca Biomedica, Padua, Italy (C.Gu., F.P., M.G., B.M., C.Ga., E.B., A.C., F.Ci., R.N., M.F., G.S., C.A.); and Departments of Pathology (F.Ca.) and Biomedical Sciences (L.B., S.G.), University of Padua, Padua, Italy

Received March 10, 2009; accepted December 2, 2009

ABSTRACT

Glycogen synthase kinase (GSK)-3 modulates the production of inflammatory cytokines. Because bleomycin (BLM) causes lung injury, which is characterized by an inflammatory response followed by a fibrotic degeneration, we postulated that blocking GSK-3 activity with a specific inhibitor could affect the inflammatory and profibrotic cytokine network generated in the BLM-induced process of pulmonary inflammation and fibrosis. Thus, here we investigated the effects of the GSK-3 inhibitor 3-(2,4-dichlorophenyl)-4-(1-methyl-1*H*-indol-3-yl)-1*H*-pyrrole-2,5-dione (SB216763) on a BLM-induced lung fibrosis model in mice. SB216763 prevented lung inflammation and the subsequent fibrosis when coadministered with BLM. Bronchoalveolar lavage fluid analysis of mice treated with BLM plus SB216763 revealed a significant reduction in BLM-induced alveolitis. Furthermore, SB216763 treatment was associated with a significantly lower production of inflammatory cytokines by macrophages. BLM-treated mice that received SB216763 developed alveolar epithelial cell damage and pulmonary fibrosis to a significantly lower extent compared with BLM-treated controls. These findings suggest that GSK-3 inhibition has a protective effect on lung fibrosis induced by BLM and candidate GSK-3 as a potential therapeutic target for preventing pulmonary fibrosis.

Idiopathic pulmonary fibrosis (IPF) is a progressive and lethal lung disease characterized by the proliferation of fibroblasts and deposition of extracellular matrix (Gross and Hunninghake, 2001). Based on several data, including the weak clinical effects of anti-inflammatory therapy on disease progression, it has been proposed that epithelial injury and activation rather than inflammation represent the key factors in the pathogenesis of IPF (Selman and Pardo, 2002; Calabrese et al., 2005). Data obtained in animal models of lung fibrosis have confirmed the importance of alveolar epithelial cell and myofibroblast cross-talk in the pathogenesis of this disease, but they have also suggested that fibrosis may be driven by the chronic inflammatory response to tissue injury (Agostini and Gurrieri, 2006). Specifically, the degree of fibrosis seems to be linked with the development of a T-cell helper 2 cell profile (Wynn, 2004).

The pulmonary fibroinflammatory response induced in mice by bleomycin (BLM) is regulated by a profibrotic

This work was supported by the Italian Ministry of University and Scientific and Technological Research [Grant Progetti di Rilevante Interesse Nazionale" N.Rd-Ra: 155.400] (to C.A.).

C.G. and F.P. contributed to this work equally.

Article, publication date, and citation information can be found at http://jpet.aspetjournals.org.
doi:10.1124/jpet.109.153049.

ABBREVIATIONS: IPF, idiopathic pulmonary fibrosis; NF-κB, nuclear factor-κB; BLM, bleomycin; GSK, glycogen synthase kinase; CREB, cAMP response element-binding protein; SB216763, 3-(2,4-dichlorophenyl)-4-(1-methyl-1*H*-indol-3-yl)-1*H*-pyrrole-2,5-dione; MCP, monocyte chemoattractant protein; TNF, tumor necrosis factor; BALF, bronchoalveolar lavage fluid; FACS, fluorescence-activated cell sorting; TUNEL, terminal deoxynucleotidyl transferase dUTP nick-end labeling; PCR, polymerase chain reaction; H&E, hematoxylin and eosin; PBS, phosphate-buffered saline.

Downloaded from jpet.aspetjournals.org at ASPET Journals on March 5, 2016

chemokine/cytokine network activated by different signal transduction pathways, including mitogen-activated protein kinases (Day et al., 2001; Matsuoka et al., 2002), the transcription factors nuclear factor-κB (NF-κB), activator protein-1, and activating transcription factor-2 (Zhang et al., 2000; Day et al., 2001). Furthermore, toll-like receptor 2 activation seems to be one of the initial critical events that triggers the release of inflammatory cytokine and chemokine secretion upon BLM challenge (Razonable et al., 2006). This suggests the possibility of using molecular modulators to attenuate lung inflammation and fibrosis induced by BLM, including NF-κB inhibitors (Inayama et al., 2006).

Recent studies have pointed to the pleiotropic serine threonine kinase glycogen synthase kinase (GSK)-3 as a crucial mediator of inflammation homeostasis. Originally involved in insulin signaling (Woodgett, 1990), over the years GSK-3 has gained importance in pathways controlling cell proliferation and survival, such as the Wnt/β-catenin and growth factor-dependent signaling cascades (Patel et al., 2004). More recently, a regulatory role of GSK-3 in the inflammatory response and cytokine production has been demonstrated. GSK-3 negatively regulates the rate of anti-inflammatory cytokine production by activated macrophages upon toll-like receptor 2-induced activation of the phosphatidylinositol 3-kinase-Akt signaling pathway (Martin et al., 2005); indeed, its blockade favors the production of anti-inflammatory cytokines over the production of other proinflammatory cytokines. The mechanism of this latter effect relies on the inhibition of GSK-3-dependent phosphorylation of the transcription factor cAMP response element-binding protein (CREB), allowing it to sequester the coactivator CREB-binding protein away from NF-κB. Consequently, it results an inhibition of NF-κB/ CREB-binding protein-mediated activation of proinflammatory cytokine gene transcription. Indeed, mice treated with GSK-3 inhibitors are protected from LPS-induced septic shock (Martin et al., 2005).

The purpose of this study was to investigate whether the fibroinflammatory response to BLM lung injury is modulated by a well characterized GSK-3 inhibitor, SB216763 (Smith et al., 2001). We show here that inhibition of GSK-3 activity significantly prevented bleomycin induced alveolitis and lung fibrosis. In particular, GSK-3 blockade affected the chemokine/cytokine inflammatory and profibrotic milieu, by hampering the production of MCP-1 and TNF-α by lung macrophages. Moreover, a significant reduction both in BLM-induced alveolar epithelial cells apoptosis and cuboidalization as well as production of fibrosis was observed. Altogether, these results provide a rationale for including GSK-3 among the potential molecular targets for the therapy of lung fibrosis.

Materials and Methods

Animal Treatment. C57BL/6N mice (12 weeks old) were purchased from Charles River Laboratories Inc. (Milan, Italy). Experimental protocols were reviewed and approved by the local Animal Care Committee of the University of Padova (Padova, Italy). In the experiments assessing bronchoalveolar lavage fluid (BALF) cellularity and FACS analysis, mice were allocated to four groups (n = 12/group) as follows: 1) intratracheal saline + vehicle (25% dimethyl sulfoxide, 25% polyethylene glycol, and 50% saline), 2) intratracheal saline + SB216763 (20 mg/kg) (Sigma-Aldrich, St. Louis, MO) dissolved in vehicle, 3) intratracheal BLM (3 U/kg) (Aventis Pharma SpA, Varese, Italy) + vehicle, and 4) intratracheal BLM + SB216763 (20 mg/kg) in vehicle. Another set of experiments to assess cytokine expression by reverse transcription-PCR (see below) was conducted in which we divided the mice (n = 12/group) to receive 1) intratracheal saline + vehicle, 2) intratracheal BLM, and 3) intratracheal BLM + SB216763. To induce pulmonary fibrosis, BLM was intratracheally administered in mice (n = 15/group) on day 0. BLM and saline-treated mice were administered with SB216763 dissolved in vehicle or vehicle alone intravenously at day 0 and then intraperitoneally twice a week until day 28. Mice were sacrificed by CO_2 inhalation on days 2, 7, and 28. In the terminal deoxynucleotidyl transferase dUTP nick-end labeling (TUNEL) experiments, the cohorts of mice were as follows: saline-treated (n = 6), BLM-treated (n = 6), and BLM + SB216763-treated (n = 6). Dimethyl sulfoxide, polyethylene glycol, and SB216763 (Smith et al., 2001) were all purchased from Sigma-Aldrich (Milan, Italy).

Histology, Special Stain, and Immunohistochemistry. Four weeks after intratracheal instillation, the mice were weighed, anesthetized, heparinized, and exsanguinated via the femoral artery. The heart and lungs were removed en bloc; the lungs were dissected away from the external vasculature and bronchi and sectioned parasagittally, superior to inferior. Liver and kidneys were also explanted, and all the specimens were fixed in buffered 4% paraformaldehyde for morphological studies. Fixed lung tissues were embedded in paraffin and stained with hematoxylin and eosin (H&E) and Masson's trichrome. The degree of inflammatory cell infiltration, of interstitial fibrosis, and of alveolar cuboidalization was evaluated using a semiquantitative subjective scoring method (as percentage of lung parenchyma involved as observed microscopically): mild, 0 to 30%; moderate, 30 to 50%; and diffuse, >50%. Heart, liver, and kidneys were also histologically processed to detect toxic pathological changes. Moreover, to precisely quantify fibrosis, formalin-fixed paraffin-embedded lung tissue were cut at 4- to 5-μm slices and stained with H&E for the evaluation of inflammatory cell infiltration and the entity of alveolar cuboidalization and with Heidenheim's trichrome for the extension of interstitial fibrosis. Then, each section was scanned at 40× magnification to identify at least five areas (hot spots) with the largest extension of fibrosis (trichrome staining). Each hot spot was then examined at 200× magnification (0.949 mm^2/field), and the fibrosis was quantified by using digital quantitative analysis (Image-Pro Plus version 4.1; Media Cybernetics, Silver Spring, MD). The mean value of the five areas was taken as representative of the whole section. Serial sections were processed immunohistochemically to investigate for the presence of GSK-3β.

After endogenous peroxidase blocking with 1% H_2O_2 in PBS, sections were treated with blocking buffer (1% fetal bovine serum in PBS and 0.3% Triton X-100 for 30 min) and incubated with a mouse anti-GSK-3β primary antibody (dilution 1:100; Santa Cruz Biotechnology, Inc., Santa Cruz, CA). After washing with PBS, tissues were exposed to biotinylated anti-mouse IgG and streptavidin peroxidase complex (Vector Laboratories, Burlingame, CA). Immunostaining was visualized with diaminobenzidine and then counterstained with hematoxylin and mounted using Poly-Mount medium (Polysciences, Warrington, PA)

Determination of Hydroxyproline. The hydroxyproline content of mouse lung was determined by standard methods as described previously (Dell'Aica et al., 2006). In brief, after rinsing with PBS, the lung was defatted, dried, weighed, and hydrolyzed for 22 h at 110°C in 6 N HCl. Aliquots were then assayed by adding chloramine-T solution for 20 min, 3.15 M perchloric acid for 5 min, and Erlich's reagent at 60°C for 20 min. Absorbance was measured at 561 nm, and the amount of hydroxyproline was determined against a standard curve. Results were expressed as

Downloaded from jpet.aspetjournals.org at ASPET Journals on March 5, 2016

percentage of collagen content (weight/weight) relative to dry weight of the tissue sample, considering that OH-Pro accounts for approximately 11.8% of the amino acid content (Dell'Aica et al., 2006).

TUNEL Assay. End labeling of exposed 3′-OH ends of DNA fragments was performed with the TUNEL in situ cell death detection kit AP (Roche Diagnostics, Indianapolis, IN) as described by the manufacturer. After staining, 20 fields of alveoli were randomly chosen for examination. The labeled cells were expressed as a percentage of total nuclei.

Lung Homogenates Preparation. Mouse lungs were minced, digested at 37°C for 1 h in a saline solution containing collagenase IV (Sigma-Aldrich), 2% fetal calf serum, and 5 mM EDTA and then filtered to obtain a cell suspension that was resuspended in buffered 30% Percoll gradient (Amersham Biosciences, Little Chalfont, Buckinghamshire, UK) and then stratified on buffered 60% Percoll gradient. After centrifugation at 500*g* for 25 min, mononuclear cells were recovered from the interface between the 30 and 60% Percoll gradients and washed three times with ice-cold PBS by centrifugation at 400*g* for 8 min. Total cell counts and viability were determined.

Bronchoalveolar Lavage. Mice were anesthetized and a soft cannula (23-gauge) was inserted into the trachea. Bronchoalveolar lavage was performed three times by the instillation and withdrawal of 0.3 ml of saline at various time points. The BALF cells were centrifuged at 400*g* for 10 min at 4°C, red blood cells were lysed, and BALF cells were then microscopically scored on a Neubauer counting chamber (PBI International, Milan, Italy).

Flow Cytometric Analysis and Cell Sorting. BALF cells were resuspended in FACS buffer (Sigma-Aldrich) and incubated with phycoerythrin- and fluorescein isothiocyanate-conjugated anti-mouse monoclonal antibody $CD3^+$, $CD4^+$, $CD8^+$, $Gr1^+$, and $Mac1^+$ (BD Biosciences Pharmingen, San Diego, CA) for 30 min at 4°C. Flow cytometry was performed after gating on the lymphocyte population using a FACSCalibur analytical flow cytometer (Immunocytometry Systems, San Jose, CA) and analyzed using CellQuest Pro software (BD Biosciences, San Jose, CA). T $CD4^+$ lymphocytes and $Mac1^+$ macrophages were double-labeled using mouse monoclonal antibody anti-$CD4^+$ and $Mac1^+$ (BD Biosciences Pharmingen) and FACS-sorted from the lung cells suspension by FACSAria cell sorter (BD Biosciences) according to the manufacturer's instructions.

RNA Isolation, Reverse Transcription, and Real-Time PCR Analysis. RNA was extracted using RNeasy mini kit (QIAGEN, Valencia, CA) according to the manufacturer's instructions. RNA was reverse-transcribed using the Reverse Transcription system (Promega, Madison, WI) according to the manufacturer's instructions. Real-time PCR reactions were carried out on an ABI PRISM 7000 sequence detection system (Applied Biosystems, Foster City, CA). Reactions were performed with SYBR Green PCR Master Mix (Invitrogen, Carlsbad, CA). β-actin was used as reference gene for the adjustment of relative expression data. All assays were performed twice to ensure their reproducibility, and a negative control was included in each run.

Real-Time PCR Primer Sequences. Primer sequences were as follows: β-actin F5′-GAGAGGGAAATTCGTGCGTA-3′ and R5′-ACATCTGCTGGAAGGGTGGC-3′; MCP-1 F5′-GCCAGCTCTC-TCTTCCTCCAC-3′ and R5′-GCGTTAACTGCATCTGGCTA-3′; and TNF-α F5′-TCTATGGCCCAGACCCTCAC-3′ and R5′-GTTTGCTACGACGTGGGCTAC-3′.

Statistical Analysis. Data are expressed as means ± S.E.M. Statistical significance was determined by one-way analysis of variance or Student's *t* test. Where needed in the case of failure of the normality tests, analyses were followed by Mann-Whitney U test or Tukey's test. For all analyses, $p < 0.05$ was accepted as statistically significant.

Results

The In Vivo Administration of the GSK-3 Inhibitor SB216763 in Mice Treated with Intratracheal BLM Is Safe and Protects from BLM-Induced Distress Respiratory Syndrome. To evaluate the effect of GSK-3 inhibition in a mouse model of lung inflammation and fibrosis, we differently randomized cohorts of C57BL6 mice to receive intratracheal instillation of either saline, saline plus the GSK-3 inhibitor SB216763, BLM plus vehicle, or BLM plus SB216763 and followed their health status for 28 days. Four of BLM-treated mice (30%) died of respiratory distress between day +14 and day +17 after the treatment. On the contrary, none of the mice receiving SB216763 intravenously at day 0 and subsequently intraperitoneally twice a week died (data not shown), suggesting that in vivo administration of SB216763 is safe. Furthermore, the coadministration of SB216763 significantly improved the survival of BLM-treated mice ($p < 0.05$; data not shown). Similarly, no deaths were observed in the group treated with saline plus SB216763 (data not shown).

Expression of GSK-3 in the Lung. Next, to determine in which lung cellular compartments GSK-3 was expressed, we analyzed the pattern of GSK-3β expression at day +28 in the lungs of control (saline) and BLM-treated mice. As shown in Fig. 1A, GSK-3β expression in the lung

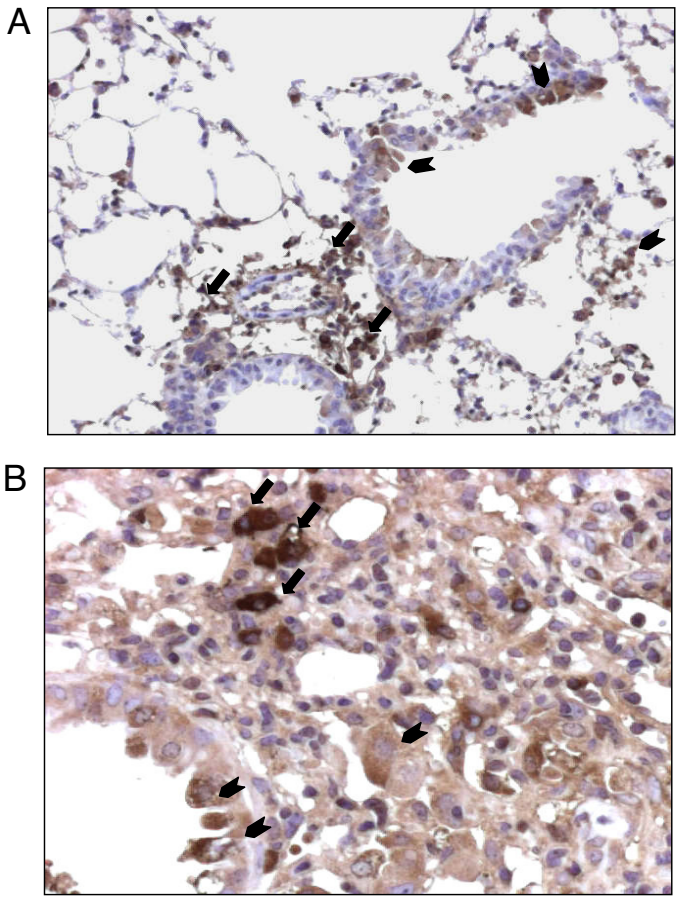

Fig. 1. Immunohistochemical analysis of GSK-3β expression in the lung of mice after 28 days from saline (A) or BLM (B) treatment. Arrows indicate lymphomonocytes and macrophages, and arrowheads indicate epithelial (bronchial and alveolar) cells. In A, the original magnification is 200×, and in B the original magnification is 400×, to better highlight the details.

Downloaded from jpet.aspetjournals.org at ASPET Journals on March 5, 2016

of healthy control mice (receiving intratracheal saline solution) was confined to some bronchial and alveolar epithelial cells as well as mucosal and interstitial lymphomonocytes, with a strong cytoplasmic staining. On the contrary, in the inflamed and fibrotic lungs of BLM-receiving mice (Fig. 1B), a strong cytoplasmic GSK-3β immunostaining was observed in most of the infiltrating lymphomonocytes and also in the alveolar cuboidalized epithelial cells. These data demonstrate that GSK-3 is expressed both in the inflammatory as well as in the epithelial cellular components of healthy and, more markedly, of injured lung.

GSK-3 Inhibition Modulates BLM-Induced Alveolitis. We then examined whether the blockade of GSK-3 could affect the dynamics of the evolution of the early phases of the inflammatory process taking place in the lung upon BLM exposure. To this aim, we analyzed the BALF obtained from saline, BLM plus vehicle, BLM plus SB216763-treated mice, at 7 days ($n = 12$ for each group) and 28 ($n = 12$ for each group) days after treatment. BLM administration caused a marked alveolitis peaking at day +7 and lasting up to day +28 as demonstrated by the microscopic score of BALF total inflammatory cells (sum of macrophages, lymphocytes, and neutrophils; Fig. 2). On the contrary, the cytological analysis of BALF of the control groups [saline or (not shown) saline plus SB216763] did not reveal a significant alveolitis, neither at day +7 nor at day +28. Remarkably, mice randomized to receive BLM plus SB216763 showed a noteworthy reduction, compared with BLM-treated mice, in the overall BALF cellularity at day +7, which was confirmed also at day +28 ($p < 0.05$).

Flow cytometry analysis of BALFs allowed a qualitative determination of the different cell populations involved in BLM-induced alveolitis, namely, macrophages ($Mac1^+$ cells), neutrophils ($Gr1^+$ and $Gr1^+/Mac1^+$ cells), and T lymphocytes ($CD3^+/CD4^+$ and $CD3^+/CD8^+$ cells). BLM treatment caused an important neutrophilic alveolitis as early as day +2 (66 ± 19%; data not shown). At day +7, the proportion of neutrophil decreased (42 ± 10%) and then at day +28 increased again (72 ± 20%; data not shown). As shown in Fig. 3A, the analysis of the ratio between activated ($Gr1^+/Mac1^+$) and nonactivated neutrophils ($Gr1^+/Mac1^-$) (Lagasse and Weissman, 1996) revealed the presence of a considerable lung infiltration of activated neutrophils at day +2 that gradually extinguished giving place to the prevalence of a nonactivated population at day +7 and, mostly, at day +28. Comparable levels of the percentage of total neutrophils were observed in the BALF of BLM-treated and BLM plus SB216763-treated mice at all the time intervals analyzed (2 days, 57 ± 29%; 7 days, 51 ± 27%; 28 days, 63 ± 5%; data not shown). However, the ratio between activated and nonactivated neutrophils was significantly reduced in the group of mice treated with BLM plus SB216763, compared with BLM-treated mice, at both day +2 and day +7 ($p < 0.05$).

Moreover, in the BLM-treated group, compared with saline-treated controls, a significant increase in the percentage of $CD3^+$ T lymphocytes at day +7 was observed and it lasted up to day +28 (Fig. 3B). SB216763 administration plus BLM, on the contrary, caused a clear and significant reduction in T lymphocyte percentage both at day +7 ($p < 0.001$) and at day +28 ($p < 0.01$). In Fig. 3C, representative FACS analysis are shown.

No significant differences were observed between the two groups in terms of $CD3^+$ T lymphocyte CD4/ CD8 ratio (data not shown). Finally, flow cytometry analysis of BALF at day +7 showed a similar increase in the percentage of $Mac1^+$ monocyte/macrophage cells in the BLM plus vehicle and BLM plus SB216763 groups, followed by a gradual decline to baseline values at day +28 (data not shown).

GSK-3 Blockade Inhibits BLM-Induced Macrophage Inflammatory Cytokine Production. To assess the effects of GSK-3 blockade on pulmonary monocytes/macrophages exposed to BLM epithelial injury, we determined the gene expression levels of two macrophage-derived molecules, TNF-α and MCP-1/CCL2, involved in the inflammatory profibrotic cascade. Analyses were performed at day +7 after BLM administration, on $Mac1^+$ monocytes/macrophages isolated from lungs of mice belonging to the various treatment cohorts ($n = 12$/group).

Administration of SB216763 to mice exposed to BLM consistently reduced the levels of TNF-α and MCP-1/CCL2 detected in $Mac1^+$ lung cells compared with mice treated

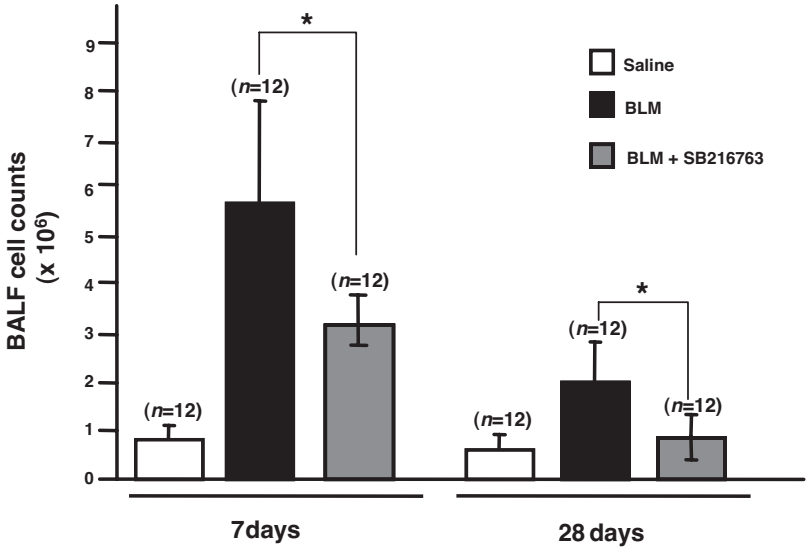

Fig. 2. SB216763 reduced the magnitude of BLM-induced alveolitis. Mice were treated with saline, BLM + vehicle, or BLM + SB216763 (20 mg/kg; $n = 12$/group) as described under *Materials and Methods*. Bronchoalveolar lavage was performed on days 7 and 28. Results represent mean ± S.D. *, $p < 0.05$, comparing BLM + SB216763-treated mice with control mice given only BLM.

Downloaded from jpet.aspetjournals.org at ASPET Journals on March 5, 2016

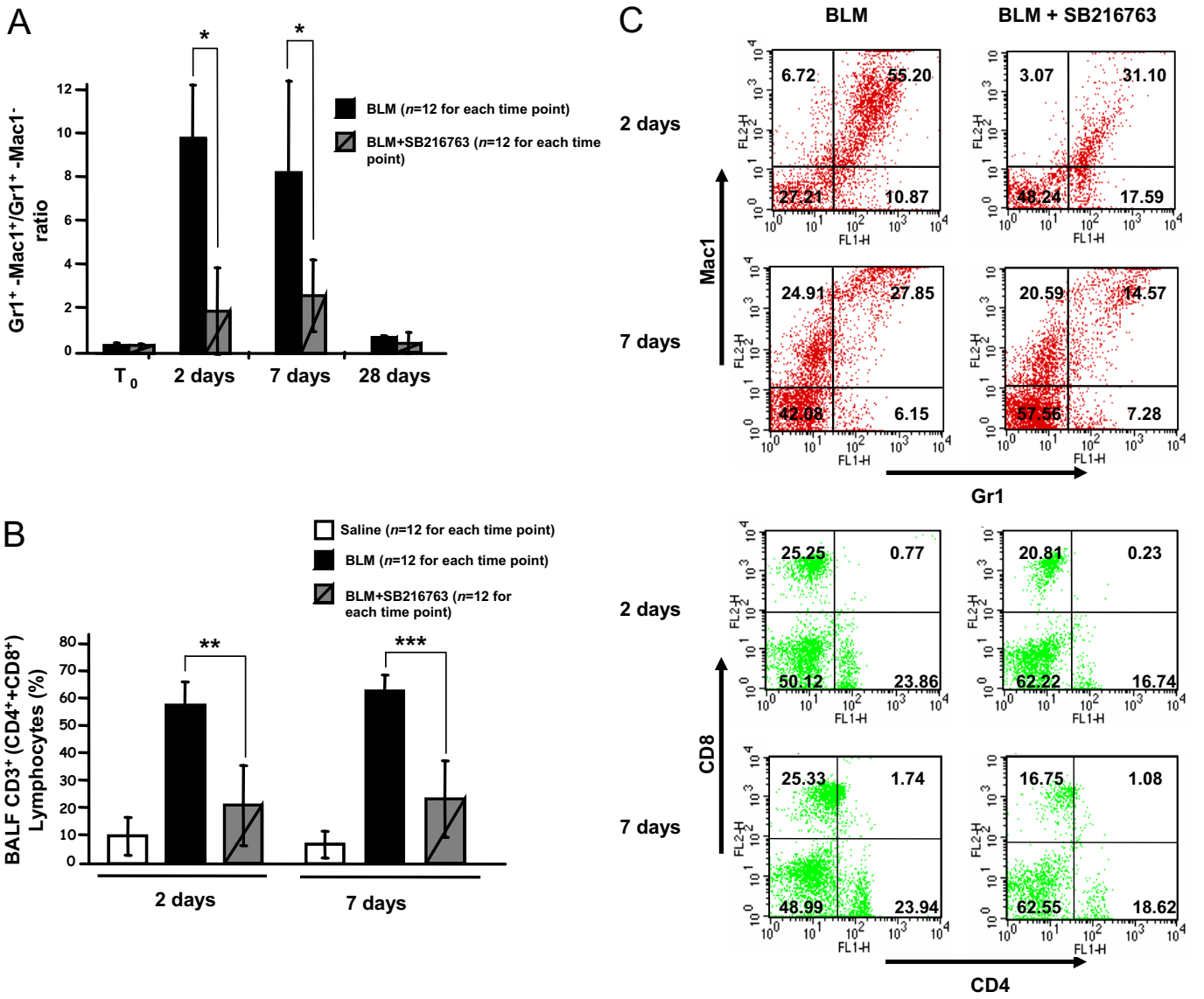

Fig. 3. SB216763 attenuated the BLM-induced inflammatory cellular infiltrate in the lung. A and B, flow cytometric analysis of BALF cells upon BLM challenge shows that SB216763 coadministration notably reduced at both days +2 and +7 the percentage of activated neutrophils ($Gr1^+$-$Mac1^+$) (A) and of $CD3^+$ ($CD4^+$ plus $CD8^+$) lymphocytes (B). C, representative dot plot graphs of the FACS analysis of the $Gr1^+/Mac1^+$ (top) and the $CD3^+$ (bottom) cells in the BLM and BLM + SB216763-treated mice. Results represent mean ± S.D. (n = 12/treatment group for each time point). *, $p < 0.05$; **, $p < 0.001$; and ***, $p < 0.01$, comparing BLM + SB216763-treated mice with control mice given only BLM.

with BLM alone ($p < 0.05$ and $p < 0.001$, respectively; Fig. 4, A and B). No relevant differences were observed between mice treated with saline or treated with saline plus SB216763 (data not shown).

GSK-3 Blockade Modulates BLM-Induced Lung Fibrosis. To determine whether the treatment with SB216763 could also have antifibrotic effects, mice treated with BLM, BLM plus SB216763 or saline were sacrificed on day +28 and subjected to histopathological examination. No differences were detected by macroscopic analysis of lungs from the different treatment groups of mice (n = 15/group). Histological evaluation on lungs from BLM-treated mice showed diffuse mononuclear cell infiltrates, epithelium cuboidalization, and alveolar septa thickening associated with collagen deposition (Fig. 5, A, D, and G). On the contrary, lungs of mice in the BLM plus SB216763 treatment arm displayed a significant reduction in inflammatory infiltrates, epithelium cuboidalization, and fibrosis (Fig. 5, B, E, and H). No alterations in the normal alveolar architecture were observed in saline-treated control groups. (Fig. 5, C, F, and I). Moreover, no microscopic degenerative changes were observed in the heart, liver, and kidney of SB216763-treated mice, thus excluding drug toxicity (data not shown). The alterations observed by the microscopical analysis in the different experimental conditions were then scored through a pathological scoring system and represented as percent of lung parenchyma involved (Fig. 6A). In addition to the histomorphometric evaluation, we also performed the quantification of the hydroxyproline (OH-Pro) content in the lungs of variously treated mice (Fig. 6B). We found that mice that received BLM had a lung OH-Pro content higher than that of saline-treated control mice and that the OH-Pro content in the lungs of mice treated with BLM plus SB216763 contained

Downloaded from jpet.aspetjournals.org at ASPET Journals on March 5, 2016

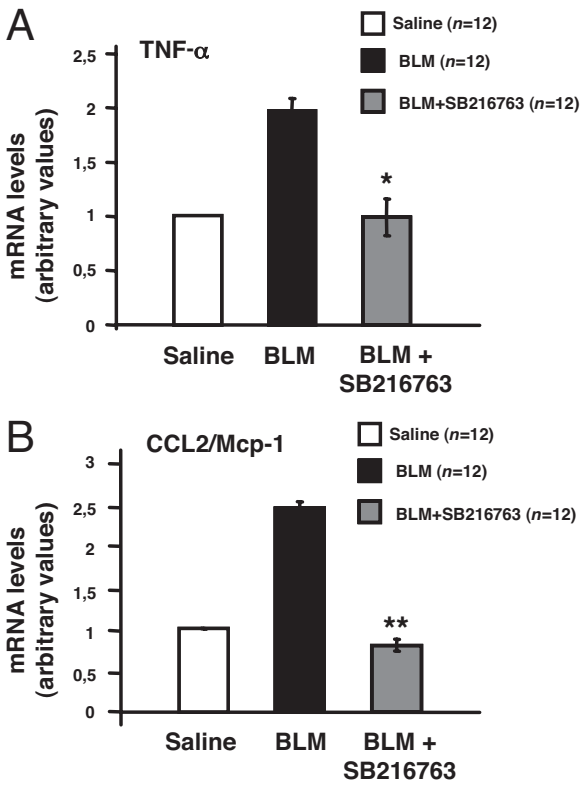

Fig. 4. SB216763 reduced BLM-induced monocytes/macrophages inflammatory cytokine expression. Real-time PCR analysis of Mac1$^+$ lung derived cells at day +7 after BLM stimulation showed an SB216763-mediated reduction in the expression levels of TNF-α (A) and MCP-1/CCL2 (B). Results represent mean ± S.D. (n = 12/treatment group). *, $p < 0.05$ and **, $p < 0.001$, comparing BLM + SB216763-treated mice with control mice given only BLM.

less OH-Pro than the lungs of mice that received BLM only [mean ± S.E.M. collagen content, saline group (n = 5), 4.8 ± 0.4%; BLM group (n = 8), 7.40 ± 0.36%; and BLM + SB216763 group (n = 7); 5.65 ± 0.19%]. The difference between BLM and saline as well as between BLM and BLM + SB216763 groups were statistically significant ($p < 0.01$). These data suggest that the pharmacological inhibition of GSK-3 leads to a decreased collagen deposition upon BLM-induced lung injury.

Moreover, we set up a series of experiments to determine the effect of GSK-3 blockade on stabilization or reduction of fibrosis after the fibrotic phase was already established compared with the effects ab initio; to this aim, mice were administered with BLM at day 0 and then the treatment with SB216763 was begun either at day 0 (n = 15; early treatment) or at day +14 (n = 15; late treatment), with subsequent twice a week administrations up to 28 days for both arms. In these experiments, to more precisely quantify the extent of fibrotic tissue, we used a semiquantitative scoring system, as detailed under *Materials and Methods*. As shown in Fig. 7, A and B, we observed a considerable reduction of fibrosis in the group of mice treated with BLM plus SB216763 compared with mice treated with BLM, and, remarkably, the antifibrotic effects present when SB216763 was administered after 14 days was comparable with that achieved with the administration of the inhibitor since day 0.

GSK-3 Inhibition Rescues Alveolar Epithelial Cells from BLM-Induced Apoptosis. Next, to test the possibility that the reduced BLM-dependent effects seen in the lungs of SB216763-treated mice could involve changes affecting the alveolar epithelial cells (which are important targets of the BLM-induced damage, as well as essential

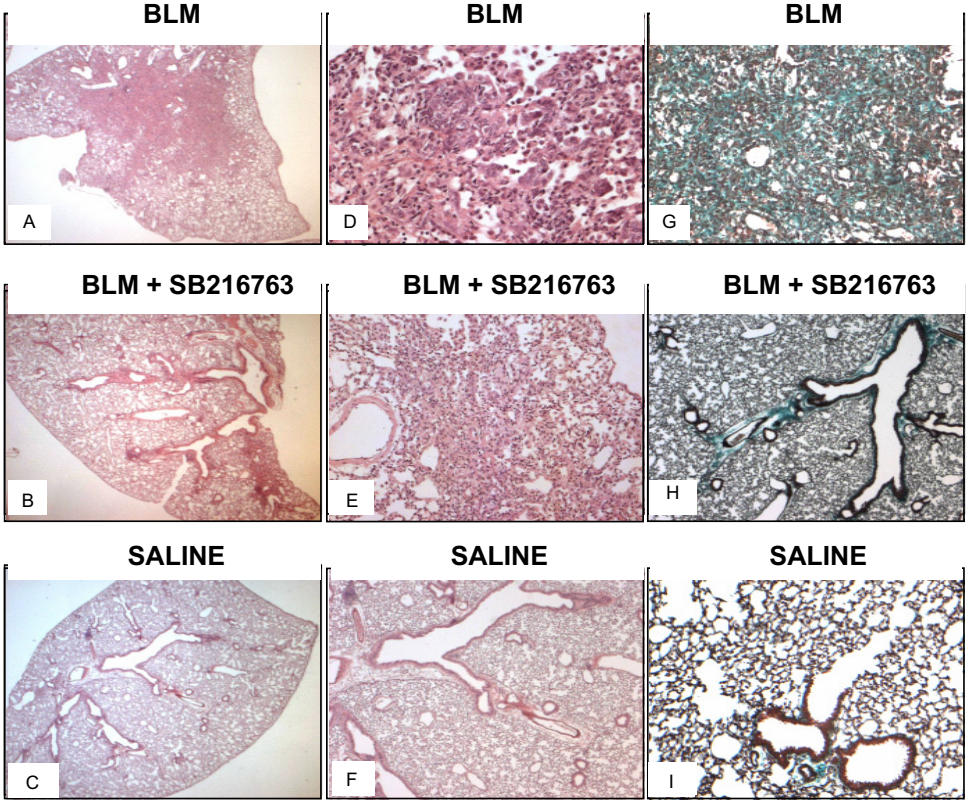

Fig. 5. Histologic examination of the lungs in BLM-induced pulmonary fibrosis. On day 28, mice treated with BLM + vehicle, BLM + SB216763, or saline were sacrificed, and histologic examination was performed by H&E staining (A–F) and Masson's trichrome staining (G–I); original magnification, 2.5× (A–C) and 100× (D–I). Mice were treated with BLM + vehicle alone (A, D, and G), BLM + SB216763 (B, E, and H), and saline (C, F, and I). As shown, lungs of mice treated with BLM + SB216763 treatment exhibited a consistent reduction in inflammatory infiltrates, epithelium cuboidalization, and fibrosis. Data are representative of three separate experiments (n = 15/treatment group).

Downloaded from jpet.aspetjournals.org at ASPET Journals on March 5, 2016

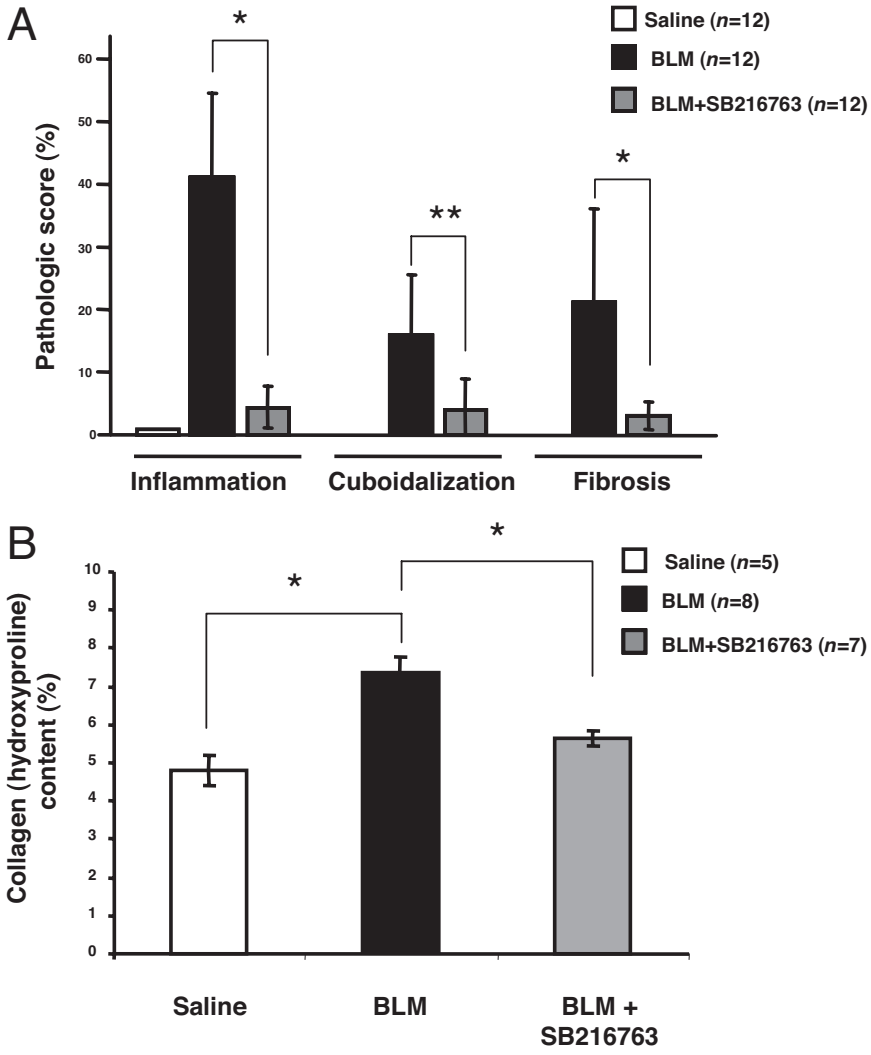

Fig. 6. A, analysis of the effects of SB216763 treatment on the lung histopathology. Graphs showing a semiquantitative evaluation (assessed by histological examination at day +28) of inflammatory cell infiltration, alveolar epithelial cells cuboidalization, and fibrosis in lungs from the different cohorts of treatment (saline, BLM + vehicle, and BLM + SB216763), which demonstrates that SB216763 administration was associated with a significant reduction in all three alterations of the lung parenchyma. Results represent mean ± S.D. (n = 15/treatment group). *, $p < 0.001$ and **, $p < 0.01$, comparing BLM + SB216763-treated mice with control mice given only BLM. B, graph showing the quantification of collagen (OH-proline) content (percentage) in the lungs of saline-treated, BLM-treated, or BLM + SB216763-treated mice. Data represent mean ± S.E.M. (n = 5 in saline-treated, 8 in BLM-treated, and 7 in BLM+SB216763-treated groups). *, $p < 0.01$, comparing saline-treated with BLM-treated mice as well as BLM + SB216763-treated with mice given only BLM.

players of the subsequent proinflammatory and profibrotic response), we evaluated the degree of cellular apoptosis upon BLM treatment in vehicle- or in SB216763-intraperitoneally injected mice; an in situ TUNEL assay was used. As shown in Fig. 8, BLM-treated control mice (n = 6) displayed a higher degree of alveolar epithelial damage compared with the BLM plus SB216763-treated mice (n = 6) that showed a significant lower amount of apoptotic alveolar epithelial cells ($p < 0.05$). These results indicate that GSK-3 is involved in BLM-induced apoptosis in alveolar epithelial cells.

Discussion

In this work, we showed that chemical inhibition of GSK-3 with a synthetic compound, SB216763, could efficiently prevent the development of BLM-induced lung fibrosis in a mouse model, likely by modulating the BLM-triggered lung damage at different levels. The most accepted view on IPF pathophysiology is based on the hypothesis that a persistent injury to the lung alveolar epithelium results in an aberrant fibrogenetic response sustained by an anomalous balance between extracellular matrix production and resorption with consequent subversion of the normal lung parenchyma architecture (Selman and Pardo, 2002; Chapman, 2004). However, the mechanisms underlying this exaggerated reparative response are unknown. A current view stresses the importance of genetic predisposition in developing IPF, and several genetic studies aimed at identifying the precise molecular determinants (Whyte, 2003; Reynolds et al., 2005) are currently ongoing. Alternatively, the role of chronic inflammatory response in IPF pathogenesis has represented a subject of intense research for many years (Shen et al., 1988; Green, 2002; Wynn, 2004). Yet, although animal models of pulmonary fibrosis clearly have shown that an inflammatory response precedes the development of fibrosis, the limited efficacy in the clinical setting of the therapeutic use of anti-inflammatory drugs in the treatment of patients affected by IPF has led to the view that the inflammatory phase represents an associated phenomenon rather than the real cause of the fibrosis development in IPF (Selman et al., 2001).

In this study, we demonstrated that the pharmacological blockade of the kinase GSK-3 markedly reduced the lung alterations (both inflammation and fibrosis) upon intratracheal administration of BLM in the mouse. Moreover, because the observed decrease in lung fibrosis in SB216763-treated mice could be due to the blunted inflammatory

Downloaded from jpet.aspetjournals.org at ASPET Journals on March 5, 2016

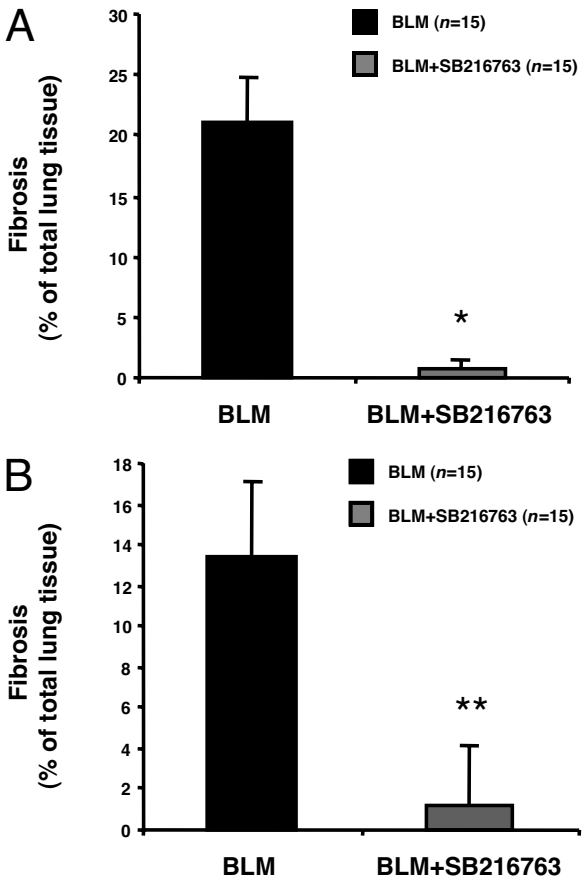

Fig. 7. Quantitative determination of fibrosis in the lungs. Mice were treated with BLM or BLM + SB216763 either starting from day 0 (A) or day +14 (B). Lungs were then processed for histological analysis, histochemistry, and collagen deposition quantification, as specified under *Materials and Methods*. Graphs show the amount of lung parenchyma involved with fibrosis in the case of BLM treatment (black bars) or BLM + SB216763 treatment (gray bars). Results represent mean ± S.D. (n = 15/treatment group). *, $p < 0.001$ and **, $p < 0.01$, comparing BLM + SB216763-treated mice with control mice given only BLM.

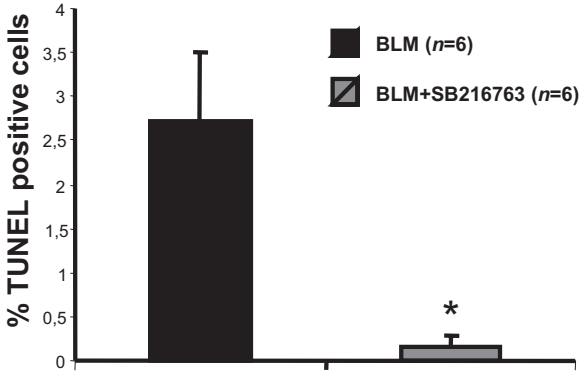

Fig. 8. In situ TUNEL analysis in the lungs. Mice were treated with BLM or BLM + SB216763 starting from day 0. At day +7, lungs were processed for in situ TUNEL analysis, and the percentage of alveolar epithelial cells was scored for specific TUNEL staining. *, $p < 0.05$ (n = 6 mice/group).

response and/or to a direct effect of the GSK-3 blockade on the mechanisms underlying fibroblast proliferation and the production of fibrotic tissue, we addressed in vivo this issue by treating mice with GSK-3 inhibitors both at the beginning (before the establishment of the inflammation) and after 14 days from BLM challenge (after the inflammation took place). In this way, we were able to dissect the effects of GSK-3 blockade in relation with the onset of inflammation and fibrosis.

Our study shows that GSK-3 inhibition is accompanied by a significant containment of the inflammation; on the other side, we provided important cues supporting the idea that GSK-3 is also likely involved in regulating the mere fibrogenetic process independently from inflammation, because its inhibition after 14 days upon lung injury (when the inflammatory process is extinguishing in large part) was still efficient in markedly reducing the onset of lung fibrosis. Lastly, we provided clear evidence that GSK-3 mediated the BLM-induced apoptosis of alveolar epithelial cells. Remarkably, we were able to demonstrate that GSK-3β is highly expressed in most of the relevant cellular compartments involved in the generation of the lung tissue damage, i.e., inflammatory cells (lymphomonocytes and macrophages), interstitial cells, and bronchial and alveolar epithelial cells.

More in details, we showed that the in vivo administration of GSK-3 inhibitor is accompanied by a reduction in the lymphocyte infiltrate and in neutrophil alveolar activation ($Gr1^+/Mac1^+$ cells) in the early phases of the inflammatory process, suggesting that GKS3 might regulate lymphocyte and neutrophil biological functions, such as cell activation, chemotaxis, and the expression of surface molecules. As a consequence, in these groups of mice, the later onset of fibrosis was markedly reduced. Moreover, GSK-3 blockade at later time points was significantly accompanied to a decrease fibrotic response compared with control mice, to an extent comparable with that seen in the experiments in which the GSK-3 inhibitor was administered at the beginning of the BLM challenge. In these series of experiments, we also observed a trend toward a decrease in the inflammatory response, which was not statistically significant. It should also be noted that the experiments evaluating the extent of fibrosis were mostly based on histomorphometric analysis and specific immunohistochemical staining of the lung, procedures that gave detailed information on the amount of lung tissue involved with the deposition of collagen. Furthermore, also when the quantification of the collagen content was addressed measuring the OH-Pro (marker-amino acid of collagen), we registered a collagen increment in the bleomycin-insulted tissues, and its reduction in the GSK-3 inhibitor-treated cases. Both the variations—increase of OH-Pro content in BLM-treated group versus saline-treated group and reduction of OH-Pro content in the BLM + SB216763-treated group versus the BLM-treated group—were statistically significant ($p < 0.01$; Fig. 6B). In addition, our finding that SB216763 partially protects alveolar epithelial cells from BLM-induced apoptosis is in agreement with the previous literature showing that GSK-3 is able to modulate apoptosis triggered by several noxae in various cell types. The role of GSK-3 in the regulation of apoptosis is, however, complex and this kinase can either protect from the extrinsic apoptotic pathway either induce the intrinsic apoptotic cascade. GSK-3 can thus operate at multiple levels in the inflammatory-fibrotic response in the lung. Mechanistically, our findings confirm recent data on the role of GSK-3 in regulating the production of proinflammatory cytokines in monocyte/macrophages (Martin et al., 2005). In partic-

Downloaded from jpet.aspetjournals.org at ASPET Journals on March 5, 2016

ular, we have demonstrated that the inhibition of GSK-3 modulates the macrophage production of TNF-α and of the chemokine CCL2/MCP1, molecules that are known to play a relevant role in the onset of the inflammatory/fibrogenetic process and in the recruitment of monocytes, respectively (Agostini and Gurrieri, 2006). Therefore, it is tempting to speculate that upon simultaneous treatment with BLM and SB216763, the reduced activation of neutrophils and the decreased recruitment of lymphocytes that we observed was a consequence of the perturbation of GSK-3-regulated macrophage functions. However, it should also be noted that there are data implicating GSK-3 in the direct regulation of cell mobility (Etienne-Manneville and Hall, 2003). In fact, in discrete subcellular compartments GSK-3 local inhibition is associated with the stimulation of cell movement (Eickholt et al., 2002; Bazzoni et al., 2005), whereas global GSK-3 inhibition inside the cell is accompanied by a profound impairment of cell mobility (Farooqui et al., 2006). However, the exact mechanisms through which GSK-3 activity influences TNF-α and MCP-1 production are unclear, but its role in regulating several transcription factors that have been shown to control the expression of these and other inflammatory genes may in part account for the observed effects. For example, GSK-3 has been shown to influence NF-κB-dependent transcription of specific target genes through a still incompletely clear mechanisms that perhaps involve the physical association of this transcription factor to DNA target sites and/or to transcriptional coactivators/corepressors. In addition, whether the reduced expression of TNF-α and MCP-1 is sufficient to affect fibroblast recruitment, activation, and proliferation and subsequent deposition of extracellular matrix is an issue deserving further investigation. Indeed, GSK-3 could also act directly on fibroblasts in the inflamed tissue or on fibrocyte-precursors in the peripheral blood. These intriguing aspects are further matter of study. Thus, the role played by this kinase could be variegate, i.e., it may orchestrate the signaling cascades involved in the initial production of inflammatory cytokines, and it may regulate the onset of fibrosis by acting at some steps of the activation of fibroblasts and of deposition of extracellular matrix. These results suggest the possibility of using GSK-3 inhibitors to modulate the inflammatory and fibrogenic response in the lung. The use of GSK-3 inhibitors has been speculated for metabolic diseases, including type II NIDDM, given the crucial role of GSK-3 downstream of insulin signaling, and some neurological conditions (bipolar disorder, Alzheimer's disease, Parkinson's disease, and Huntington's disease), because GSK-3 phosphorylates proteins playing an important pathogenetic role in these disorders. Very recently, several studies have demonstrated the potential usefulness of this approach in some inflammatory conditions. For example, mice treated with SB216763 were protected by lipopolysaccharide-induced septic shock (Martin et al., 2005). Another study showed that GSK-3 may regulate interleukin-10 production upon interferon-γ stimulation in macrophages and its inhibition leads to increased interleukin-10 levels and protection against the damage consequent to experimentally induced arthritis and peritonitis (Hu et al., 2006). Our study is the first to test the effects of GSK-3 inhibition on the development of lung inflammation and fibrosis in a mouse model, demonstrating a protective effect of this treatment.

In conclusion, by demonstrating that GSK-3 kinase regulates the lung damage upon BLM both by acting in the early phases of inflammatory cell activation and recruitment as well as at later time points in the occurrence of fibrosis, this study contributes to understanding the molecular mechanisms underlying the pathogenesis of lung inflammation and fibrosis. It is more important to note that the present data suggest that the modulation of GSK-3 may represent a novel way to improve the therapeutic options able to block fibrogenesis in diffuse lung diseases.

Acknowledgments

We thank Samuela Carraro and Gino Chioetto (Department of Clinical and Experimental Medicine, University of Padua Medical School), Dr. Filippo Naso (Department of Experimental Biomedical Sciences, University of Padua Medical School) for analytical assistance, and Dr. Martin E. Donach for assistance in editing the manuscript.

References

Agostini C and Gurrieri C (2006) Chemokine/cytokine cocktail in idiopathic pulmonary fibrosis. *Proc Am Thorac Soc* **3:**357–363.

Bazzoni G, Tonetti P, Manzi L, Cera MR, Balconi G, and Dejana E (2005) Expression of junctional adhesion molecule-A prevents spontaneous and random motility. *J Cell Sci* **118:**623–632.

Calabrese F, Giacometti C, Rea F, Loy M, and Valente M (2005) Idiopathic interstitial pneumonias: Primum movens: epithelial, endothelial or whatever. *Sarcoidosis Vasc Diffuse Lung Dis* **22:**S15–S23.

Chapman HA (2004) Disorders of lung matrix remodeling. *J Clin Invest* **113:**148–157.

Day RM, Yang Y, Suzuki YJ, Stevens J, Pathi R, Perlmutter A, Fanburg BL, and Lanzillo JJ (2001) Bleomycin upregulates gene expression of angiotensin-converting enzyme via mitogen-activated protein kinase and early growth response 1 transcription factor. *Am J Respir Cell Mol Biol* **25:**613–619.

Dell'Aica I, Sartor L, Galletti P, Giacomini D, Quintavalla A, Calabrese F, Giacometti C, Brunetta E, Piazza F, Agostini C, et al. (2006) Inhibition of leukocyte elastase, polymorphonuclear chemoinvasion, and inflammation-triggered pulmonary fibrosis by a 4-alkyliden-β-lactam with a galloyl moiety. *J Pharmacol Exp Ther* **316:**539–546.

Eickholt BJ, Walsh FS, and Doherty P (2002) An inactive pool of GSK-3 at the leading edge of growth cones is implicated in Semaphorin 3A signaling. *J Cell Biol* **157:**211–217.

Etienne-Manneville S and Hall A (2003) Cdc42 regulates GSK-3beta and adenomatous polyposis coli to control cell polarity. *Nature* **421:**753–756.

Farooqui R, Zhu S, and Fenteany G (2006) Glycogen synthase kinase-3 acts upstream of ADP-ribosylation factor 6 and Rac1 to regulate epithelial cell migration. *Exp Cell Res* **312:**1514–1525.

Green FH (2002) Overview of pulmonary fibrosis. *Chest* **122:**334S–339S.

Gross TJ and Hunninghake GW (2001) Idiopathic pulmonary fibrosis. *N Engl J Med* **345:**517–525.

Hu X, Paik PK, Chen J, Yarilina A, Kockeritz L, Lu TT, Woodgett JR, and Ivashkiv LB (2006) IFN-gamma suppresses IL-10 production and synergizes with TLR2 by regulating GSK3 and CREB/AP-1 proteins. *Immunity* **24:**563–574.

Inayama M, Nishioka Y, Azuma M, Muto S, Aono Y, Makino H, Tani K, Uehara H, Izumi K, Itai A, et al. (2006) A novel IkappaB kinase-beta inhibitor ameliorates bleomycin-induced pulmonary fibrosis in mice. *Am J Respir Crit Care Med* **173:**1016–1022.

Lagasse E and Weissman IL (1996) Flow cytometric identification of murine neutrophils and monocytes. *J Immunol Methods* **197:**137–150.

Martin M, Rehani K, Jope RS, and Michalek SM (2005) Toll-like receptor-mediated cytokine production is differentially regulated by glycogen synthase kinase 3. *Nat Immunol* **6:**777–784.

Matsuoka H, Arai T, Mori M, Goya S, Kida H, Morishita H, Fujiwara H, Tachibana I, Osaki T, and Hayashi S (2002) A p38 MAPK inhibitor, FR-167653, ameliorates murine bleomycin-induced pulmonary fibrosis. *Am J Physiol Lung Cell Mol Physiol* **283:**L103–L112.

Patel S, Doble B, and Woodgett JR (2004) Glycogen synthase kinase-3 in insulin and Wnt signalling: a double-edged sword? *Biochem Soc Trans* **32:**803–808.

Razonable RR, Henault M, and Paya CV (2006) Stimulation of toll-like receptor 2 with bleomycin results in cellular activation and secretion of pro-inflammatory cytokines and chemokines. *Toxicol Appl Pharmacol* **210:**181–189.

Reynolds HY, Gail DB, and Kiley JP (2005) Interstitial lung diseases–where we started from and are now going. *Sarcoidosis Vasc Diffuse Lung Dis* **22:**5–12.

Selman M, King TE, Pardo A, American Thoracic Society, European Respiratory Society, and American College of Chest Physicians (2001) Idiopathic pulmonary fibrosis: prevailing and evolving hypotheses about its pathogenesis and implications for therapy. *Ann Intern Med* **134:**136–151.

Selman M and Pardo A (2002) Idiopathic pulmonary fibrosis: an epithelial/fibroblastic cross-talk disorder. *Respir Res* **3:**3.

Downloaded from jpet.aspetjournals.org at ASPET Journals on March 5, 2016

Shen AS, Haslett C, Feldsien DC, Henson PM, and Cherniack RM (1988) The intensity of chronic lung inflammation and fibrosis after bleomycin is directly related to the severity of acute injury. *Am Rev Respir Dis* **137:**564–571.

Smith DG, Buffet M, Fenwick AE, Haigh D, Ife RJ, Saunders M, Slingsby BP, Stacey R, and Ward RW (2001) 3-Anilino-4-arylmaleimides: potent and selective inhibitors of glycogen synthase kinase-3 (GSK-3). *Bioorg Med Chem Lett* **11:**635–639.

Whyte MK (2003) Genetic factors in idiopathic pulmonary fibrosis: transforming growth factor-beta implicated at last. *Am J Respir Crit Care Med* **168:**410–411.

Woodgett JR (1990) Molecular cloning and expression of glycogen synthase kinase-3/factor A. *EMBO J* **9:**2431–2438.

Wynn TA (2004) Fibrotic disease and the T(H)1/T(H)2 paradigm. *Nat Rev Immunol* **4:**583–594.

Zhang XY, Shimura S, Masuda T, Saitoh H, and Shirato K (2000) Antisense oligonucleotides to NF-kappaB improve survival in bleomycin-induced pneumopathy of the mouse. *Am J Respir Crit Care Med* **162:**1561–1568.

Address correspondence to: Dr. Carlo Agostini, Department of Clinical and Experimental Medicine, University of Padova, Via Giustiniani 2, 35128 Padova, Italy. E-mail: carlo.agostini@unipd.it

Downloaded from jpet.aspetjournals.org at ASPET Journals on March 5, 2016